2023 European Control Conference (ECC)
June 13-16, 2023. Bucharest, Romania

Synchronization in Networks of Anticipatory Agents

Bengi Dönmez[1] and Fatihcan M. Atay[2]

***Abstract*— We consider a coupled Kuramoto system composed of agents that anticipate the future states of their neighbors based on past data and try to align their states accordingly. We show that this anticipatory behavior results in multiple synchronized solutions at different collective frequencies and different stability characteristics. We derive an exact condition for the stability of the synchronized states. We show that the system can exhibit multistability, converging to different synchronized solutions depending on the initial conditions.**

I. Introduction

Coupled oscillator models are frequently used to study interacting periodic processes or oscillatory systems. Among these is the celebrated Kuramoto model [1], [2]

$$\dot{\theta}_i(t) = \omega_i + \frac{K}{n}\sum_{j=1}^{n}\sin(\theta_j(t) - \theta_i(t)) \tag{1}$$

representing a system of n oscillators, where $\theta_i(t) \in S^1$, $i = 1, \ldots, n$, is the phase of oscillator i having intrinsic frequency ω_i and K is the coupling strength. If the oscillators are identical, $\omega_i = \omega$ $\forall i$. In (1) every oscillator is coupled to every other, that is, the coupling is global. One can also consider local coupling of identical oscillators:

$$\dot{\theta}_i(t) = \omega + \frac{K}{d_i}\sum_{j=1}^{n}a_{ij}\sin(\theta_j(t) - \theta_i(t)) \tag{2}$$

where $a_{ij} = 1$ if oscillator i is connected to j and zero otherwise, and $d_i = \sum_{j=1}^{n} a_{ij}$ is the number of connections (neighbors) of oscillator i. More generally, an existing connection can be given a weight by allowing a_{ij} to assume a positive value; d_i is then the sum of the weights of connection to oscillator i. In (2), the oscillators try to align their phases with the phases of their neighbors, the differences acting as a forcing to the system, and the sine function accounting for the fact that the phase differences are on the circle S^1. This extra forcing disappears when the system *synchronizes*, that is, all phases are identical, $\theta_i = \theta_j$ $\forall i, j$. It follows that the synchronized state satisfies

$$\theta_i(t) = \omega t + \phi, \quad \forall i = 1, \ldots, n \tag{3}$$

for some ϕ, that is, the oscillators exhibit periodic behavior at their intrinsic frequency ω. Moreover, it is easy to show that this synchronized state is locally stable (up to a shift ϕ) whenever the network is connected and $K > 0$.

[1]Bengi Dönmez is with the Department of Mathematics, Bilkent University, 06800 Ankara, Turkey bengi.donmez@bilkent.edu.tr

[2]Fatihcan M. Atay is with the Department of Mathematics, Bilkent University, 06800 Ankara, Turkey f.atay@bilkent.edu.tr

In this paper, we consider (2) with identical oscillators who anticipate the future states of their neighbors and align themselves accordingly. In other words,

$$\dot{\theta}_i(t) = \omega + \frac{K}{d_i}\sum_{j=1}^{n}a_{ij}\sin(\hat{\theta}_j(t+\tau) - \theta_i(t)) \tag{4}$$

where $\hat{\theta}_j(t+\tau)$ represents the predicted future state of oscillator j at time $t+\tau$, $\tau > 0$. This model is motivated by the anticipatory consensus algorithm introduced in [3] to speed up convergence to consensus. There, the prediction of the future is done by a first-order linear approximation from the past and the present states:

$$\begin{aligned}\hat{\theta}_j(t+\tau) &= \theta_j(t) + \frac{\theta_j(t) - \theta_j(t-\tau)}{\tau}\tau \\ &= 2\theta_j(t) - \theta_j(t-\tau),\end{aligned}$$

obtained by approximating the derivative at time t with a finite difference. Using this estimate in (4), we arrive at

$$\dot{\theta}_i = \omega + \frac{K}{d_i}\sum_{j=1}^{n}a_{ij}\sin(2\theta_j(t) - \theta_j(t-\tau) - \theta_i(t)), \tag{5}$$

which will the object of study in this paper. The system (5) is a set of coupled delay-differential equations, where the delay parameter τ is interpreted as the prediction horizon of the anticipatory agents.

In the following sections, we study model (5) and and investigate the effects of anticipation on synchronization. Specifically, we show that anticipation leads to multiple synchronized solutions at frequencies different from the intrinsic frequency ω, with different stability characteristics. We derive exact conditions for the local stability of the synchronized solutions in an undirected network. The stability condition turns out to be independent of the connection topology in an undirected connected network.

II. Preliminaries from Graph Theory

We briefly review some relevant notions and notations from graph theory. For details, the reader is referred to standard texts such as [4] or [5].

A graph $G = (V, E)$ consists of a finite set V of vertices and a set of edges $E \subset V \times V$ consisting of unordered pairs of vertices. Two vertices i and j are called *neighbors* if $(i, j) \in E$. We consider simple, non-trivial, and undirected graphs without self-loops or multiple edges. We denote by $A = [a_{ij}]$ the (weighted) adjacency matrix of the graph, where $a_{ij} = a_{ji} > 0$ if i and j are neighbors, and $a_{ij} = 0$ otherwise. The degree d_i of node i is defined as $d_i = \sum_{j=1}^{n} a_{ij}$, i.e., the sum of the elements of the ith row of A, and $D = \mathrm{diag}(d_1, \ldots, d_n)$ denotes the diagonal matrix of vertex degrees.

The normalized Laplacian matrix is defined as

$$L = I_n - D^{-1}A, \tag{6}$$

where n is the number of nodes in the network and I_n is the identity matrix of size n. The normalized Laplacian naturally arises in a class of important problems, in particular in random walks on networks, for which $D^{-1}A$ is the transition matrix for probability distributions arising from such walks. Although L need not be symmetric, it is similar to a real symmetric matrix, namely,

$$\begin{aligned} D^{\frac{1}{2}}LD^{-\frac{1}{2}} &= D^{\frac{1}{2}}(I_n - D^{-1}A)D^{-\frac{1}{2}} \\ &= D^{\frac{1}{2}}I_nD^{-\frac{1}{2}} - D^{\frac{1}{2}}D^{-1}AD^{-\frac{1}{2}} \\ &= I_n - D^{-\frac{1}{2}}AD^{-\frac{1}{2}}. \end{aligned}$$

Therefore, the eigenvectors of L form a complete set that spans $\mathbb{R}^n$, and the eigenvalues λ_i are real and can be ordered as

$$0 = \lambda_1 \leq \lambda_2 \leq \cdots \leq \lambda_n \leq 2, \tag{7}$$

where the bounds follow from an application of Gershgorin's theorem [6]. In particular, the upper and lower bounds imply that

$$|1 - \lambda_i| \leq 1, \quad i = 1, 2, \ldots, n. \tag{8}$$

The first eigenvalue λ_1 is always zero and corresponds to the eigenvector $v_1 = (1, 1, \ldots, 1)^\top$. The second eigenvalue λ_2, also called the *spectral gap*, is positive if and only if the graph is connected. In fact, the multiplicity of the zero eigenvalue equals the number of connected components of the graph.

III. Synchronized Solutions

Based on (3), we seek synchronized solutions of the form

$$\theta_i = \Omega t + \phi, \quad \forall i = 1, \ldots, n. \tag{9}$$

Substituting (9) into (5), it is seen that the collective synchronized frequency Ω satisfies the algebraic equation

$$\Omega = \omega + K\sin(\Omega\tau) \tag{10}$$

We first show that this equation always has a solution.

Lemma 3.1: Equation (10) has at least one solution Ω.

Proof: The statement is clear for $K = 0$. For $K \neq 0$, we rewrite (10) as

$$\frac{\Omega - \omega}{K} - \sin(\Omega\tau) = 0 \tag{11}$$

Consider the continuous and bijective function $g : \mathbb{R} \to \mathbb{R}$ defined by $g(\Omega) = \frac{\Omega - \omega}{K}$. For a fixed nonzero τ, the function $h(\Omega) := \sin(\Omega\tau)$ is continuous with range $[-1, 1]$. Since h is bounded, there exists number a and b such that $g(a) - h(a) > 0$ and $g(b) - h(b) < 0$. By Intermediate Value Theorem there exist an $\Omega^* \in (a, b)$ such that $g(\Omega^*) - h(\Omega^*) = \frac{\Omega^* - \omega}{K} - \sin(\Omega^*\tau) = 0$. ■

Unlike the standard Kuramoto model (2), system (5) with anticipating agents can have more than one synchronized

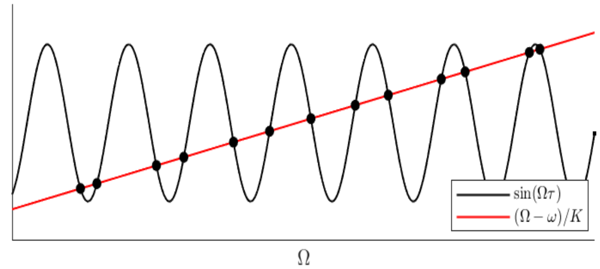

Fig. 1. Graphical solution to equation (10) for $K > 0$. The intersection points of the two curves, indicated by black dots, correspond to equilibrium solutions.

solution. Indeed, (11) can have multiple solutions for the common frequency Ω since its right hand side is oscillatory but the left hand side is monotone in Ω, as illustrated in Figure 1. This situation may cause the existence of more than one stable solution, i.e. multistability for the system, where different initial states converge to different synchronized solutions. The stability of these solutions is investigated in the next section.

IV. Stability of Synchronized Solutions

We give an exact condition for the stability of synchronized solutions (9) at frequency Ω.

Theorem 4.1: Consider system (5) on an undirected and connected network. Then the synchronized state (9), with a frequency Ω that satisfies (10), is locally exponentially stable if and only if

$$0 < \tau K \cos(\Omega\tau) < 1. \tag{12}$$

Proof: Consider perturbations $u_i(t)$ around the synchronized state (9), that is,

$$\theta_i(t) = \Omega t + \phi + u_i(t).$$

Substituting into (4) and neglecting higher order terms give the linear variational equation for small perturbations $u_i(t)$:

$$\dot{u}_i = \frac{\beta}{d_i}\sum_{j=1}^{n} a_{ij}(2u_j(t) - u_j(t-\tau) - u_i(t)),$$

where $\beta = K\cos(\Omega\tau)$. In matrix form,

$$\dot{u} = \beta[D^{-1}A(2u(t) - u(t-\tau)) - u(t)] \tag{13}$$

with $u = (u_1, u_2, \ldots, u_n)^\top$. Since $L = I - D^{-1}A$ has a full set of eigenvectors v_i that span $\mathbb{R}^n$, u can be written as a linear combination,

$$u(t) = \sum_{i=1}^{n} \alpha_i(t)v_i \tag{14}$$

where $Lv_i = \lambda_i v_i$ and $\alpha_i = \langle u^i, u\rangle$, with u^i being the left eigenvectors of L [6], [7]. As a result, (13) transforms into n decoupled scalar differential equations

$$\dot{\alpha}_i(t) = \beta[(1 - 2\lambda_i)\alpha_i(t) - (1 - \lambda_i)\alpha_i(t-\tau)] \tag{15}$$

for which the characteristic equation is

$$\psi_i(s) := s - \beta[(1 - 2\lambda_i) - (1 - \lambda_i)e^{-s\tau}] = 0.$$

Thus, the characteristic equation for the system (13) can be written as the product

$$\Psi(s) := \prod_{i=1}^{N} \psi_i(s) = \prod_{i=1}^{N} [s - \beta[(1-2\lambda_i) - (1-\lambda_i)e^{-s\tau}] = 0.$$

The local stability of the synchronized solution is thus equivalent to all roots of Ψ having negative real parts, except for a simple root at zero, corresponding to neutral perturbations along the synchronization subspace spanned by $v_1 = (1, 1, \dots, 1)^\top$. We will show that the condition $0 < \tau K \cos(\Omega\tau) < 1$ is necessary and sufficient for Ψ to have a single root at zero, corresponding to the zero Laplacian eigenvalue, and all other roots with negative real parts.

The first factor in Ψ, related to $\lambda_1 = 0$, is

$$\psi_1(s) = s - \beta(1 - e^{-s\tau}).$$

One can observe that $\psi_1(0) = 0$ and $\psi_1'(0) = 1 - \beta\tau \neq 0$ provided $\beta\tau \neq 1$. By a change of variable $s' = s\tau$, the stability of ψ_1 is equivalent to the stability of

$$\bar{\psi}_1(s') = s' - \beta\tau(1 - e^{-s'}).$$

By a classical result due to Hayes [8], the function $s - a_1 - a_2 e^{-s}$ has a simple root at $s = 0$ and all other roots have negative real parts if and only if coefficients satisfy $-a_2 = a_1 < 1$. Therefore, $\bar{\psi}_1(s')$, and thus ψ_1, has a simple root at 0 and all other roots have negative real parts if and only if $\beta\tau < 1$. In particular, $\beta\tau < 1$ is a necessary condition for the stability of Ψ.

The remaining roots come from the rest of the characteristic equation given by $\prod_{i=2}^{N} \psi_i(s) = 0$. Hence, the characteristic roots satisfy

$$s - \beta[(1 - 2\lambda_i) - (1 - \lambda_i)e^{-s\tau}] = 0, \quad i = 2, \dots, n. \quad (16)$$

We next show that $\beta\tau > 0$ is a necessary condition for the roots of (16) to have negative real parts. Indeed, since the Laplacian eigenvalues λ_i are nonnegative, we have

$$(1 - 2\lambda_i) \leq (1 - \lambda_i).$$

The condition $\beta\tau \leq 0$ would thus imply

$$\tau\beta(1 - 2\lambda_i) \geq \tau\beta(1 - \lambda_i),$$

and by [8, Theorem 1], (16) would then have a solution s with $\mathrm{Re}(s) \geq 0$. Therefore, $\beta\tau > 0$ is necessary for stability.

Having established the necessary conditions $\beta\tau < 1$ and $\beta\tau > 0$, it remains to show that all roots of (16) have negative real parts under the condition $0 < \beta\tau < 1$. Now observe that if $\tau = 0$, then (16) gives

$$s = -\beta\lambda_i < 0, \qquad i = 2, \dots, n; \qquad (17)$$

therefore, in the absence of delays, all roots are negative. Since roots change continuously with the parameter τ, we look at possible loss of stability by imaginary axis crossing

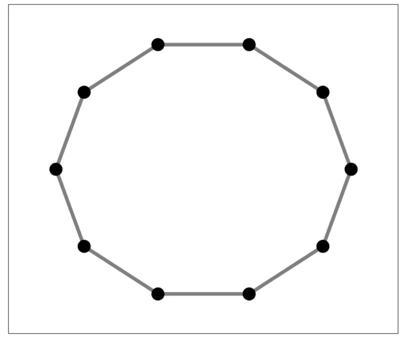

Fig. 2. Cyclic network on 10 vertices.

of roots for $\tau > 0$. Hence, putting $s = i\gamma$ for some $\gamma \in \mathbb{R}$ into (16) and considering the imaginary parts gives

$$\begin{aligned}\gamma &= \mathrm{Im}(\beta(1 - 2\lambda_i) - \beta(1 - \lambda_i)e^{-i\gamma\tau}) \\ &= \beta(1 - \lambda_i)\sin(\gamma\tau)\end{aligned}$$

Therefore,

$$|\gamma| \leq |\beta(1 - \lambda_i)\gamma\tau|. \qquad (18)$$

since $|\sin x| \leq |x| \; \forall x \in \mathbb{R}$. Note that $\gamma \neq 0$ since otherwise $s = 0$ would be a solution of (16), which is not possible since $\lambda_i > 0$ for $i \geq 2$ and $\beta > 0$. Hence we can divide (18) by $|\gamma|$ and use (8) to obtain

$$1 \leq |\tau\beta(1 - \lambda_i)| \leq |\tau\beta| = \tau\beta$$

as the condition for the existence of a purely imaginary root. Therefore, if $\beta\tau < 1$, then the characteristic roots cannot cross the imaginary axis, and so they all have negative real parts. This completes the proof of the theorem. ■

V. Numerical Illustrations

A. Stable and unstable synchronized solutions

For numerical simulations, we take the intrinsic frequency of the oscillators to be $\omega = 1$ and coupling strength $K = 1$. To illustrate Theorem 4.1, we consider (5) on a cyclic network with 10 vertices, as shown in Figure 2. For $\tau = 1.2$, equation (10) has a unique solution $\Omega \approx 1.8187$. By Theorem 4.1, the corresponding synchronized solution is unstable. Figure 3 shows that the phases of diverge from one another with time even though the initial phases are chosen to be very close. On the other hand, for $\tau = 0.3$ the system has a synchronous solution with frequency $\Omega \approx 1.4107$, and Theorem 4.1 implies that this solution is stable. Simulation results in Figure 4 show that even under significant perturbations, the agents converge to a common solution.

B. Multistability

For numerical calculations we use a complete undirected graph with $n = 4$ vertices, as shown in Figure 5.

We set $\tau = 0.7$, the intrinsic frequency $\omega = 0.2$, and coupling strength $K = 2$. With this choice of parameters, there are three synchronized solutions in the form (9). The solutions of the (10) giving the collective frequencies Ω are depicted in Figure 6. Using Theorem 4.1, we find that two

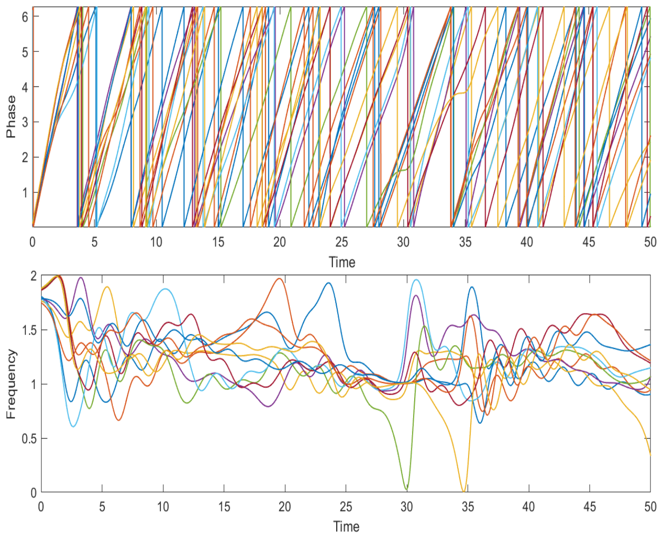

Fig. 3. Time evolution the oscillators phases and frequency with $\tau = 1.2$, showing that the system does not synchronize.

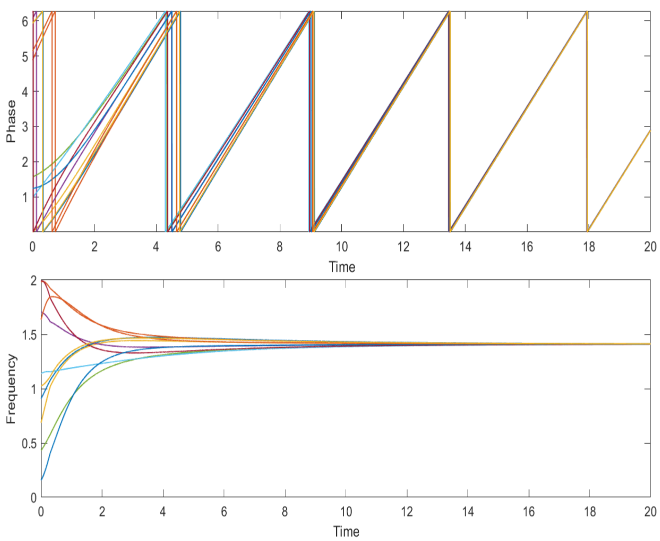

Fig. 4. Time evolution of the oscillators' phases, showing convergence to a synchronized solution at frequency $\Omega \approx 1.4107$.

of the synchronized solutions are stable and one solution is unstable. For different initial conditions, solutions converge to different stable states, as shown in Figure 7.

VI. Synchronization versus Consensus

If the sine function in (5) is replaced by the identity function and the parameters are chosen as $\omega = 0$ and $K = 1$, then one obtains the anticipatory consensus problem considered in [3], namely

$$\dot{\theta}_i = \frac{1}{d_i} \sum_{j=1}^{n} a_{ij} (2\theta_j(t) - \theta_j(t-\tau) - \theta_i(t)). \qquad (19)$$

Consensus in (19) refers to the agents' states converging to a common value ϕ. In this sense, consensus can be identified with a synchronized solution in (5) of the form (9) with $\Omega = 0$. Theorem 4.1 then gives the synchronization

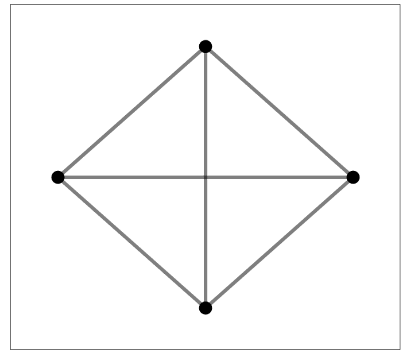

Fig. 5. Complete network on 4 vertices.

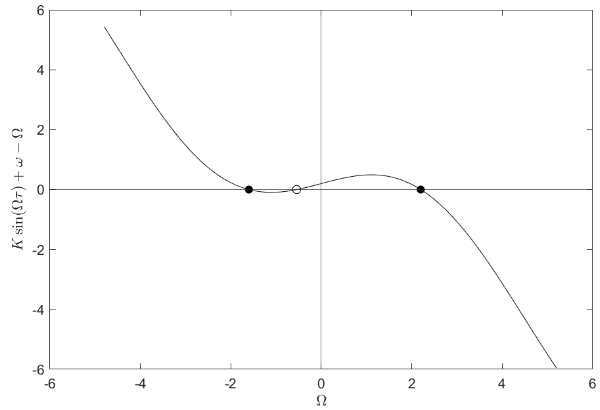

Fig. 6. Three solutions for the collective frequency Ω. Black dots correspond to stable solutions at $\Omega \approx -1.6005$ and $\Omega \approx 2.1990$. The white dot corresponds to an unstable synchronized solution.

condition as $0 < \tau < 1$, which is the same as the consensus condition given by Theorem 3 in [3]. However, at different parameter values, the stability conditions are not identical, and the oscillator system (5) may admit a stable synchronized solution whereas the consensus solution is unstable in (19).

To illustrate, we take $\tau = 1.5$. Since $\tau > 1$, the consensus state in (19) is unstable [3, Theorem 3]. However, with $K = 1$ and $\omega = 0.1$, the oscillator system (5) has a stable synchronized solution at frequency $\Omega \approx -0.8614$, as calculated from (10). The situation is illustrated in simulations in Figure 8 for an all-to-all coupled network of size $n = 10$.

One can understand the mechanism of the difference by comparing the respective stability conditions in the two systems. Indeed, the stability condition (12) for the synchronized solution from Theorem 4.1 now reads

$$0 < \tau \cos(\Omega\tau) < 1 \qquad (20)$$

as opposed to the consensus condition

$$\tau < 1 \qquad (21)$$

Due to the presence of the cosine factor in (20), which can be smaller than one, it may be possible to satisfy condition (20) even when (21) fails. In other words, it may be possible to obtain synchronization in the nonlinear system (5) for values of τ that are too large for the linear system (19) to converge to a common consensus value. Considered together

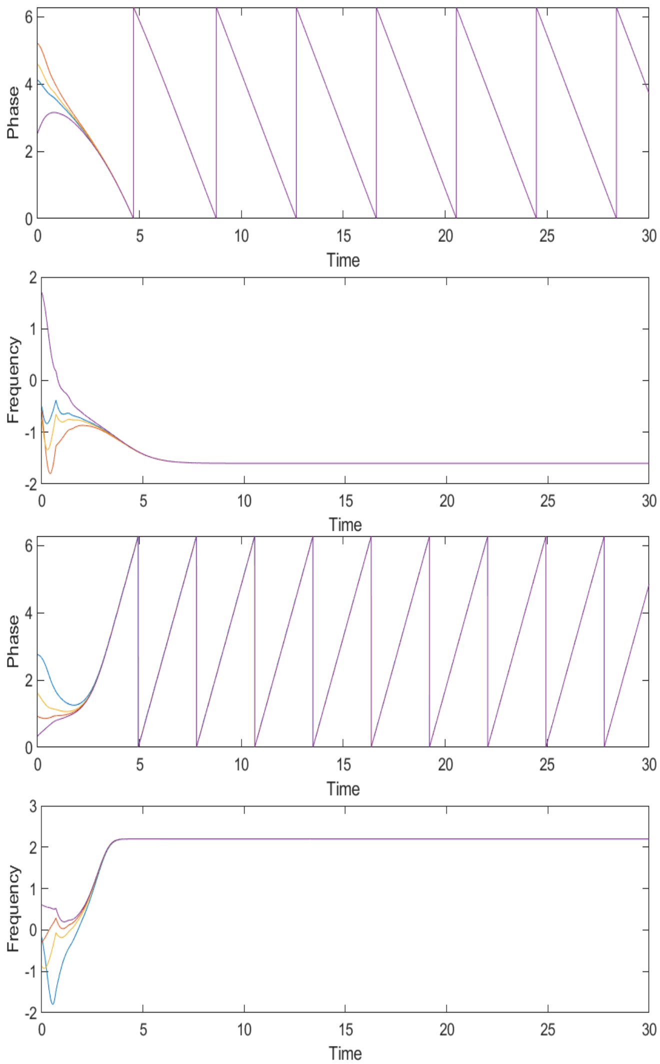

Fig. 7. Multistability of synchronized states starting from different initial conditions. In the first simulation (top two plots) the oscillators converge to a common frequency $\Omega \approx -1.6005$. In the second simulation (bottom two plots), starting from different initial conditions, the oscillators converge to a common frequency $\Omega \approx 2.1990$. The values of the frequencies are the same as shown in Figure 6.

with the possibility of multiple synchronized solutions and multistability, as seen in the previous sections, the Kuramoto oscillator model (5) of anticipatory agents offers a much richer source of dynamical behavior.

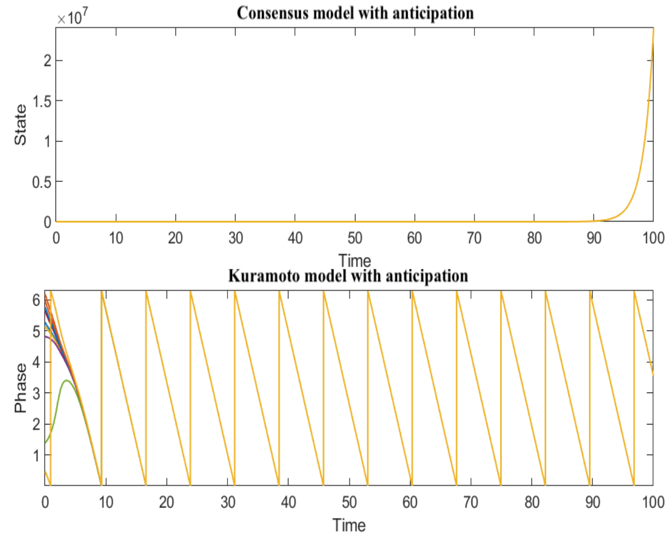

Fig. 8. Time evolution of the consensus model (19) and the Kuramoto model (5), both of anticipatory agents, starting from the same initial conditions. Although the consensus problem diverges (top figure), the Kuramoto system synchronizes (bottom figure).

VII. Conclusion

We have considered a coupled system of identical Kuramoto oscillators where oscillators anticipate the future states of their neighbors and try to align their phases to the estimated future. We have shown that such anticipatory behavior can result in the birth of multiple synchronized states at different collective frequencies and having different stability properties. We have given an exact condition for the local asymptotic stability of the synchronized state. Stability depends on the various parameters of the system, including the prediction horizon τ and the collective frequency, but does not depend on the network structure. We have presented numerical simulations supporting the theoretical results and exhibiting new phenomena such as multistability and emphasized the differences with the linear consensus problem.

In closing, we note that the stability condition presented in Theorem 4.1 of this paper pertains to undirected networks and does not necessarily apply to directed networks. In particular, for directed networks, the stability of the synchronized state may depend on the network topology in a significant way. This was also observed for the original anticipatory consensus problem previously [9].

References

[1] Y. Kuramoto, “Self-entrainment of a population of coupled non-linear oscillators,” in *International Symposium on Mathematical Problems in Theoretical Physics*, H. Araki, Ed. Berlin, Heidelberg: Springer Berlin Heidelberg, 1975, pp. 420–422.

[2] ——, *Chemical Oscillations, Waves, and Turbulence*. Berlin: Springer, 1984.

[3] F. M. Atay and D. Irofti, “A delayed consensus algorithm in networks of anticipatory agents,” in *2016 European Control Conference (ECC)*. IEEE, jun 2016, pp. 1880–1885. [Online]. Available: https://doi.org/10.1109/ecc.2016.7810565

[4] F. R. K. Chung, *Spectral Graph Theory*, ser. CBMS Regional Conference Series in Mathematics. American Mathematical Society, Providence, RI, 1997, vol. 92.

[5] C. Godsil and G. Royle, *Algebraic Graph Theory*. New York: Springer-Verlag, 2001.

[6] F. M. Atay, “The consensus problem in networks with transmission delays,” *Philos. Trans. R. Soc. Lond. Ser. A Math. Phys. Eng. Sci.*, vol. 371, no. 1999, pp. 20 120 460, 13, 2013. [Online]. Available: http://dx.doi.org/10.1098/rsta.2012.0460

[7] ——, “On the duality between consensus problems and Markov processes, with application to delay systems,” *Markov Processes and Related Fields*, vol. 22, no. 3, pp. 537–553, 2016. [Online]. Available: http://math-mprf.org/journal/articles/id1433/

[8] N. D. Hayes, “Roots of the transcendental equation associated with a certain difference-differential equation,” *J. London Math. Soc.*, vol. 25, pp. 226–232, 1950.

[9] D. Irofti and F. M. Atay, “On the delay margin for consensus in directed networks of anticipatory agents,” *IFAC-PapersOnLine*, vol. 49, no. 10, pp. 206–211, 2016, 13th IFAC Workshop on Time Delay Systems TDS 2016. [Online]. Available: https://doi.org/10.1016/j.ifacol.2016.07.530